Overview of LH operation at JET

K. K. Kirov, A. Ekedahl, J. Bernardo, M. Goniche, J. Mailloux, M. F. F. Nave, and

Citation: AIP Conference Proceedings **1689**, 080001 (2015);
View online: https://doi.org/10.1063/1.4936524
View Table of Contents: http://aip.scitation.org/toc/apc/1689/1
Published by the American Institute of Physics

Overview of LH Operation at JET

K. K. Kirov[1, a)], A. Ekedahl[2], J. Bernardo[3], M. Goniche[2], J. Mailloux[1], M. F. F. Nave[3] and JET Contributors*

EUROfusion Consortium, JET, Culham Science Centre, Abingdon, OX14 3DB, UK.
[1]CCFE Fusion Association, Culham Science Centre, Abingdon, United Kingdom
[2]CEA, IRFM, F-13108 Saint-Paul-Lez-Durance, France
[3]Inst. de Plasmas e Fusão Nuclear, Inst. Superior Tecnico, Univ. de Lisboa, Lisbon, Portugal
** See the Appendix of F. Romanelli et al., Proc. of the 25th IAEA Fusion Energy Conference, 2014, Saint Petersburg, Russia*
[a)] Corresponding Author: Krassimir.Kirov@ccfe.ac.uk

Abstract. In this report key aspects of Lower Hybrid Current Drive (LHCD) operation at JET are presented. Amplitude and broadening of the Radio Frequency (RF) spectrum at about 3.7GHz and the frequency shift of the lower sideband were analyzed by means of new diagnostic utilizing RF spectra measurements. Dependencies on plasma density, LH power and the toroidal magnetic field were studied. Plasma rotation profiles with and without LH power were investigated. Power deposition and Current Drive (CD) profiles were assessed by means of a new Ray Tracing / Fokker Planck (RT/FP) code. Significant progress in a number of technological issues including the new supplementary arc protection system based on a visible camera imaging system and operation of the system with waveguides filled with N2 instead of greenhouse SF6 gas was achieved.

INTRODUCTION

Following the successful installation of ILW on JET [1], a relatively trouble-free operation of the LHCD system up to 3MW of coupled microwave power in L-mode plasma has been achieved [2]. JET programme in 2013-14 was mainly focused on scenario development in support of urgent ITER needs. LHCD was used in studies related to plasma current control and *q*-profile optimization in Advanced Tokamak (AT) scenario development. Furthermore, a new LH-related diagnostic based on RF spectra measurements was setup, tested and validated during JET restart. Initial data have been collected and analyzed in order to address important issues regarding the impact of the Parametric Decay Instabilities (PDI) [3, 4] on the CD efficiency at high densities. In addition a new RT/FP code was developed at JET in order to study the impact of the real plasma shape and poloidal variations in the launched spectrum on the LH wave power deposition and CD efficiency. Section 1 of the paper summarizes main results on LH physics while in Section 2 improvements of the arc protection system and initial operation with waveguides filled with N2 are reported.

RF PHYSICS

RF Spectra Measurements

The RF spectrum in the LH range of frequencies was measured on JET by (*i*) a new diagnostic using a magnetic loop, 2.5cm x 4.5cm, outside (~1m) of JET vessel; and (*ii*) from the reflected RF power from one of the transmission lines on the middle row.

It is well known [3, 4] that the spectral broadening of the launched LH (pump) wave at 3.7GHz is caused by scattering from low frequency density fluctuations at the plasma edge, while lower sideband appearance can be related to parametric decay of the pump wave into another LH wave (the lower sideband) and a low frequency

Radio Frequency Power in Plasmas
AIP Conf. Proc. 1689, 080001-1–080001-4; doi: 10.1063/1.4936524

quasimode. The amplitude, A, of the main peak at f_0=3.7GHz, its half width, δf, at -30dB from A, low sideband peak, A_{LS}, and frequency shift, Δf_{LS}, relative to f_0, Fig. 1(a), were analyzed versus the launched LH power, P_{LH}, line averaged plasma density, $\bar{n}_e$, and magnetic field, B_T. The accuracy in frequency measurements has been assessed of the order of 0.06MHz, while the natural LH spectrum at 3.7GHz is very narrow, δf_0<0.1MHz. Example RF spectra from reflected power data (red) and RF probe (blue) are presented in Fig. 1(a). While the main peak in both cases was centered at 3.7GHz the signal from the reflected power was found stronger and in general broader.

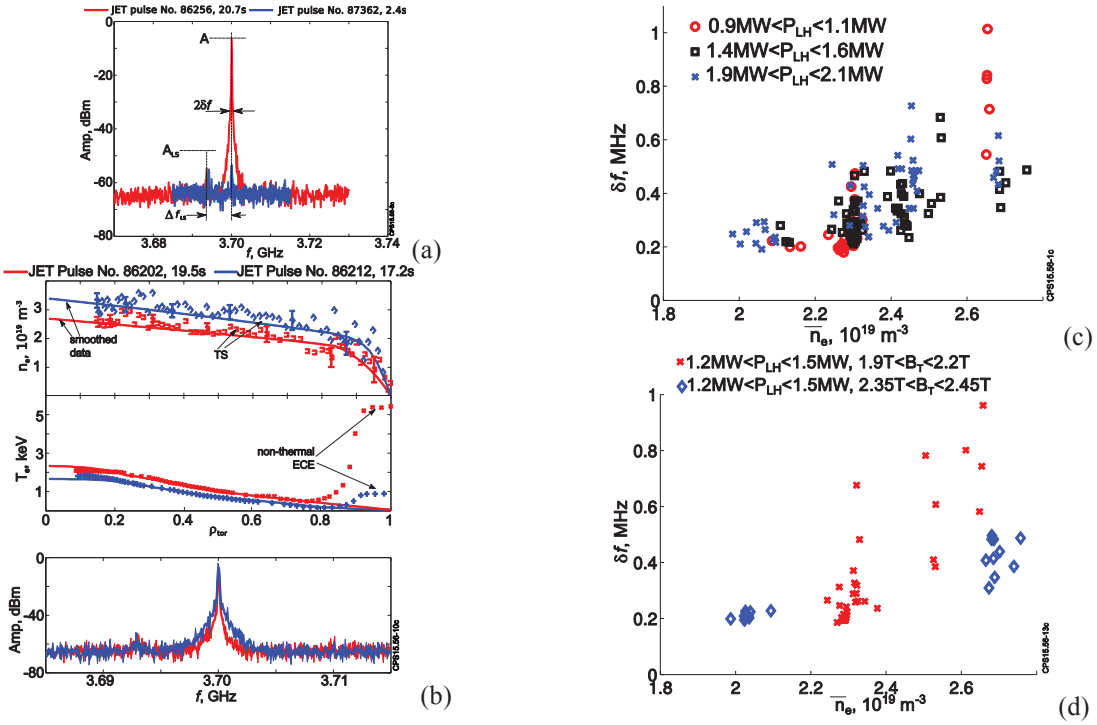

FIGURE 1. (a) RF spectra from reflected power data (#86256, 20.7s, in red) and RF probe (#87362, 2.4s, in blue); (b) Comparison between low (#86202, 2.37T/1.8MA, in red) and high density (#86212, 2.42T/1.8MA, in blue) JET pulses. The RF spectra are at the bottom graph. Density and electron temperature from Thomson Scattering (TS) are indicated with squares and diamonds, Electron Cyclotron Emission (ECE) temperature is shown in 'x' and '+' and the solid lines are the smoothed profiles; (c) RF spectra broadening, δf, versus line averaged density, $\bar{n}_e$ for low (red circles), intermediate (black squares) and high (blue crosses) P_{LH}; (d) RF spectra broadening, δf, versus $\bar{n}_e$ for low (red x) and high (blue diamonds) B_T. P_{LH} is between 1.2 and 1.5MW. All data in (b), (c) and (d) were taken from reflected power measurements.

Two pulses at similar configuration and different density are shown in Fig. 1(b). In the case with higher density (in blue) the LH wave accessibility was reduced to the plasma periphery on the LFS, while the broadening of the main peak was larger, Fig. 1(b) bottom. The CD efficiency also decreased as seen from the non-thermal ECE data. This can be interpreted as a result of more intense scattering of the LH wave on the density perturbations.

A large database related to the RF spectra was collected and analyzed. The main plasma and LH parameters were in the following ranges: 1.95T<B_T<2.45T, 1.27×10^{19}m^{-3}< $\bar{n}_e$<2.90×10^{19}m^{-3}, 0.5MW<P_{LH}<2.7MW. It was found that the normalized main peak maximum A[W]/P_{LH}[W] does not change with P_{LH} but the low sideband peak A_{LS}[W]/P_{LH}[W] decreases with P_{LH}. The width of the main peak δf always increases with density independently on P_{LH} and B_T (Fig. 1(c), (d)). This was accompanied by (*i*) decrease in the fast electrons population as deduced from the non-thermal ECE and (*ii*) a reduction in LH wave accessibility. For lower magnetic field the increase in δf was stronger with density, Fig. 1(d). It was also observed that δf decreases with increasing density profile peaking, measured as $n_e(\rho=0.2)/n_e(\rho=0.8)$. Low sideband frequency shift was always at about 7MHz with very little scatter of the data, ≈1MHz, i.e. $\Delta f_{LS} \approx 7 \pm 1$ MHz. Ion cyclotron frequency for D in the region of interest was about 14-15MHz for ~2.4T pulses. In the pulses analyzed here $T_e \approx T_i$ can be assumed and for the two cases shown in Fig. 1(b) f_0/f_{LH}>5 was found, meaning that the low sideband cannot be related to parametric decay in this case. It was assessed that PDI can be observed at JET for $\bar{n}_e$>3×10^{19}m^{-3}, which was not achieved in this experiment.

Intrinsic Plasma Rotation with LHCD

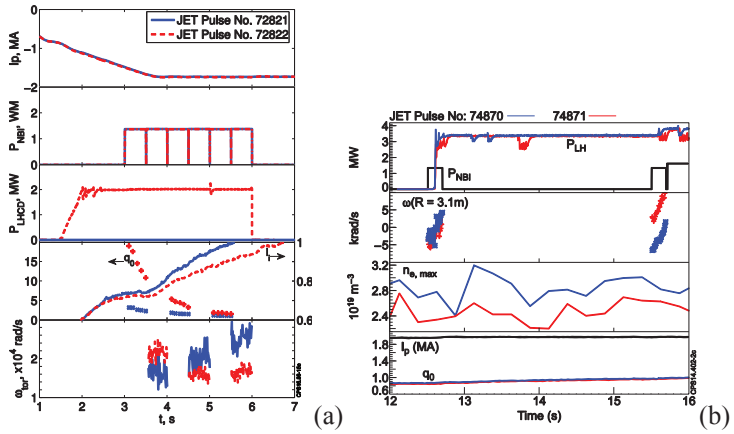

FIGURE 2. (a) Time traces of I_p, P_{NBI}, P_{LH}, q_0, l_i and $\omega_{tor}(R_0=3.05m)$ in LH (red) and non-LH (blue) preheat JET pulses; (b) time traces of P_{NBI}, P_{LH}, $\omega_{tor}(R_0=3.1m)$, n_e, I_p and q_0 for a pulse with the typical core-counter rotation (blue) and an exception with core co-rotation (red).

The effect that LHCD has on plasma rotation has been studied in two types of experiments [5]:

- plasmas with LHCD added to NBI heating, Fig. 2(a).
- LHCD-only plasmas for measurement of intrinsic rotation, Fig.2 (b).

Both cases showed that LHCD has a clear impact on the rotation. The typical intrinsic rotation profile with LHCD showed co-current rotation in the edge, with counter rotation in the core. In a few exceptions the core was co-rotating. What determines the direction of rotation is still under investigation.

Changes from co- to counter-rotation as the q-profile evolves (Fig. 2(a)) from above unity to below unity, suggests that magnetic shear could be important. The effect that the LH wave's deposition profile might have on rotation was assessed. The differences between peaked and hollow rotation profiles were not correlated with changes in LH accessibility. It has been found that core co-rotation increases with LH power as the latter changes from 1.3 to 4.2 MW [5].

New RT/FP Code for LH Wave Propagation and CD studies

A new JET RT/FP code, JRT, was developed. It accounts for the proper 2D geometry of the plasma and the launcher and can be run with different power and $N_{||}$ spectrum of the launched LH wave for each row of the grill. The new RT code is also more portable and can be used with a number of FP solvers. Disadvantages are that the code cannot treat caustics properly, which is a common issue for RT codes in LH frequency range. RT part of the code is validated versus GENRAY code [6], while 1D FP results were tested against LCS code.

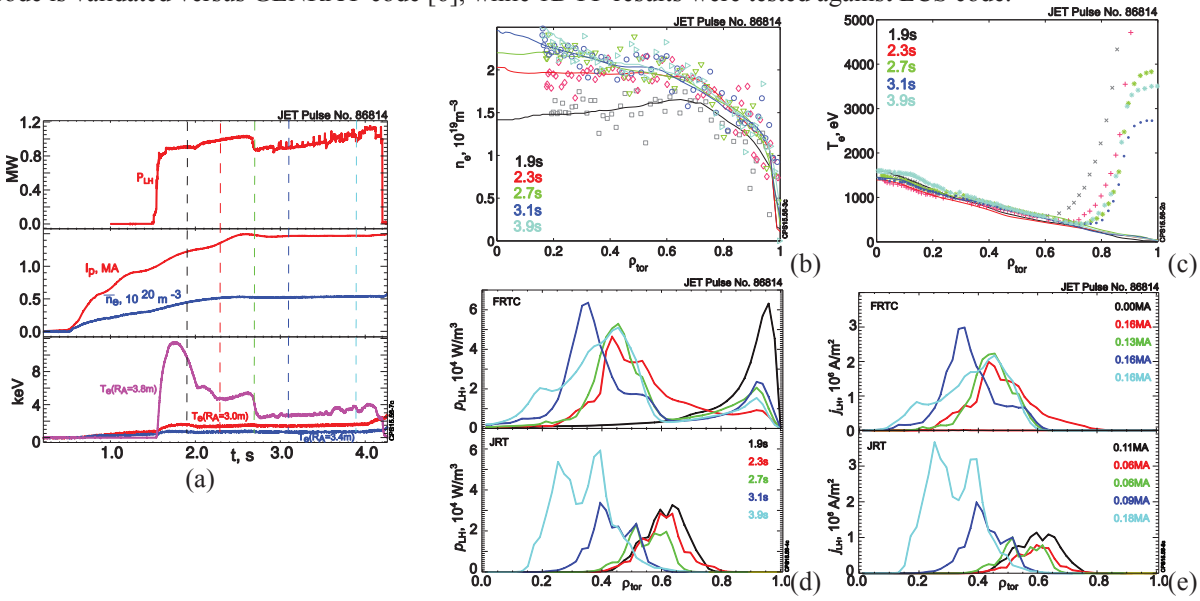

FIGURE 3. (a) Time traces of AT scenario pulse #86814, 2.4T/1.5MA, with n_e and T_e profiles at five time slices in (b) and (c); (d) Power deposition profiles from the new code JRT compared to FRTC at the five time intervals; (e) LH current drive for JRT and FRTC. The total driven current at each time slice is provided for comparison.

Results from LHCD simulations of JET AT scenario pre-heat phase are shown in Fig. 3. The existing FRTC code [7], which uses simple geometry and LH wave spectrum, predicted significant collisional absorption for ρ_{tor}>0.8 at the first instant, Fig. 3(d) (black curve), while JRT calculated about 0.11MA of driven current, which is in qualitative agreement with observed suprathermal emission from ECE. At the last time slice the two codes predicted off-axis power deposition and CD profiles. The total driven current was assessed to be 0.16MA by FRTC and 0.18MA by JRT.

LH OPERATIONS

New Arc Protection System Based on Visible Camera Imaging.

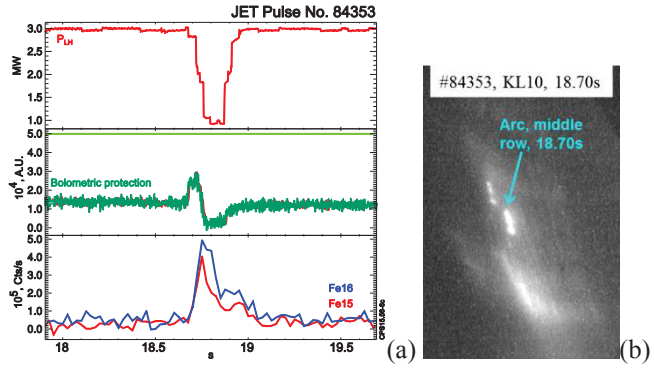

FFIGURE 4. (a) Time traces of PLH, radiation protection signal and Fe15, Fe16; (b) arc as seen on KL10 camera in the middle of the grill. Arc has been quickly quenched in time to prevent large influx of Fe and disruption, as shown in (a).

Visible camera data was used in addition to the existing imbalance protection system to protect against arcs at the launcher mouth. The protection required real-time processing of the image sequence from KL10 camera. A total of 24 Regions Of Interest (ROIs) were assigned to sections of the LH launcher fed by individual klystrons. Dedicated software was developed to process the data and pass the information to the local manager, which acts on the arcing klystron(s). $D_{\alpha,\beta}$ filter was used to avoid image being overwhelmed by ionization light.

Light in ROI(s) is interpreted as arc(s) and the protection trips the klystron(s) feeding these parts of the grill. Figure 4 gives an example where the new protection based on the visible camera imaging successfully quenched an arc at the launcher mouth and prevented further damage to the launcher and large amount of impurities entering the vessel.

Operation with N2

Up to now LH transmission lines were filled with SF6 gas, which is an excellent isolator regarding HV breakdown but also a harmful green-house gas. A project aiming at replacing SF6 in the waveguides with N2 has been started and the initial results were very encouraging. One transmission line, corresponding to A1 klystron, has been tested successfully with N2 at 2 Bar gauge pressure and with RF power, 466kW/10sec in test load and 260kW/5sec in launcher with plasma. The whole LHCD system is being certified to operate with N2 at up to 2Bar gauge pressure.

ACKNOWLEDGEMENTS

This work has been carried out within the framework of the Contract for the Operation of the JET Facilities and has received funding from the European Union's Horizon 2020 research and innovation programme. The views and opinions expressed herein do not necessarily reflect those of the European Commission.

REFERENCES

1. G. Matthews et al., 2011, Phys. Scr. 014001.
2. K. K. Kirov et al., 2013, Plasma Phys. Controll. Fusion 115008.
3. M. Porkolab and R. P. H. Chang, 1978, Review Mod Phys, p.745.
4. R. Cesario et al., 2010, Nat. Commun. 1:55, doi:10.1038/ncomms1052
5. M. F. F. Nave et al., 2015, Nucl. Fusion, in preparation
6. A. Smirnov, R. Harvey and K. Kupfer, 1994, Bull Amer. Phys. Soc. Vol 39, No. 7, p. 1626 Abstract 4R11
7. A. R. Esterkin and A. D. Piliya, 1996, Nucl. Fusion, p. 1501